# Reconfigurable Intelligent Surfaces in 6G: Reflective, Transmissive, or Both?

Shuhao Zeng, *Graduate Student Member, IEEE*, Hongliang Zhang, *Member, IEEE*, Boya Di, *Member, IEEE*, Yunhua Tan, *Member, IEEE*, Zhu Han, *Fellow, IEEE*, H. Vincent Poor, *Life Fellow, IEEE*, and Lingyang Song, *Fellow, IEEE*

***Abstract*— Reconfigurable intelligent surfaces (RISs) have attracted wide interest from industry and academia since they can shape the wireless environment into a desirable form at low cost. In practice, RISs have three types of implementations: 1) reflective, where signals can be reflected to the users on the same side of the base station (BS), 2) transmissive, where signals can penetrate the RIS to serve the users on the opposite side of the BS, and 3) hybrid, where the RISs have a dual function of reflection and transmission. Most existing works focus on the reflective type RISs, and the other two types of RISs have not been well investigated. In this letter, a downlink multi-user RIS-assisted communication network is considered, where the RIS can be one of these types. We derive the system sum-rate, and discuss which type can yield the best performance under a specific user distribution. Numerical results verify our analysis.**

***Index Terms*— Reconfigurable intelligent surfaces, sum-rate analysis, type selection.**

## I. Introduction

THE recent development of meta-surfaces has given rise to a new technology, reconfigurable intelligent surfaces (RISs), which can control the wireless communication environment and improve the signal quality at receivers [1]. The RIS is an ultra-thin surface inlaid with many sub-wavelength units, whose electromagnetic (EM) responses can be tuned via onboard positive-intrinsic-negative (PIN) diodes. According to the energy split for reflection and transmission, the RISs can be roughly categorized into three types: reflective, transmissive [2], and hybrid [3], [4]. Specifically, the reflective type RIS reflects incident signals towards the users on the same side of the base station (BS) while signals can penetrate the transmissive type RIS towards the users on the opposite side of the BS. For the hybrid type, the RIS enables a dual function of reflection and transmission.

Most exisiting studies in the literature focus on the reflective type RIS. For example, in [5], a point-to-point orthogonal frequency division multiplexing network assisted by a reflective type RIS was studied, where the authors proposed a practical transmission protocol to estimate channels and optimize reflection successively. In [6], two efficient channel estimation schemes were proposed for different channel settings in a reflective type RIS-assisted multi-user network with orthogonal frequency division multiple access. In [7], a multi-user network assisted by a reflective type RIS was investigated, where the digital beamformer at the BS and RIS configurations were jointly optimized to maximize the sum rate.

In this letter, we consider an RIS-assisted downlink multi-user network with one BS, where the RIS can be any one of the three types. We first derive an upper bound on the system sum-rate, based on which the optimal type of RIS under different user equipment (UE) distributions is then discussed. Finally, simulation results verify the validity of our derivation and the proposed optimality conditions.

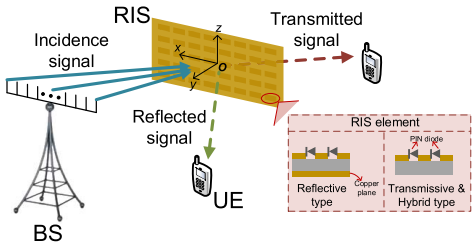


Fig. 1. System model of an RIS-assisted cellular network.

## II. System Model

### A. Scenario Description

As shown in Fig. 1, we consider a downlink multi-user communication system, which consists of a BS equipped with $K_t$ antennas and $S$ UEs each having a single antenna. Due to the unexpected fading and potential obstacles, the links from the BS to the UEs may fall into complete outage. To alleviate this issue, we deploy an RIS to assist the communication, which reflects or penetrates the signals from the BS towards the UEs by shaping the propagation environment into a desirable form. To describe the topology of the network, we introduce Cartesian coordinates, where the *x*-*z* plane coincides with the RIS, and the origin is located in the center of the RIS. The regions $y < 0$ and $y > 0$ are referred to as the *transmission zone* and *reflection zone*, respectively. Furthermore, we use $\mathcal{S}_R$ and $\mathcal{S}_T$ to represent the set of UEs that are located in the reflection zone and transmission zone, respectively, with the number of such UEs denoted by $S_R$ and $S_T$, respectively. Therefore, we have $S = S_T + S_R$.

### B. Reconfigurable Intelligent Surfaces

An RIS is composed of $M \times N$ sub-wavelength elements, each with the size of $l_M \times l_N$. As shown in Fig. 1, each element has several PIN diodes onboard. When the biased

Manuscript received February 10, 2021; accepted February 22, 2021. Date of publication February 26, 2021; date of current version June 10, 2021. This work was supported in part by the National Natural Science Foundation of China under Grants 61625101, 61829101, and 61941101, and in part by the U.S. National Science Foundation under Grants EARS-1839818, CNS-1717454, CNS-1731424, CNS-1702850, and CCF-1908308. The associate editor coordinating the review of this letter and approving it for publication was C. You. *(Corresponding author: Lingyang Song.)*

Shuhao Zeng, Yunhua Tan, and Lingyang Song are with the Department of Electronics, Peking University, Beijing 100871, China (e-mail: shuhao.zeng@pku.edu.cn; tanggeric@pku.edu.cn; lingyang.song@pku.edu.cn).

Hongliang Zhang and H. Vincent Poor are with the Department of Electrical Engineering, Princeton University, Princeton, NJ 08544 USA (e-mail: hongliang.zhang92@gmail.com; poor@princeton.edu).

Boya Di is with the Department of Computing, Imperial College London, London SW7 2AZ, U.K. (e-mail: diboya92@gmail.com).

Zhu Han is with the Department of Electrical and Computer Engineering, University of Houston, Houston, TX 77004 USA, and also with the Department of Computer Science and Engineering, Kyung Hee University, Seoul 02447, South Korea (e-mail: zhan2@uh.edu).

Digital Object Identifier 10.1109/LCOMM.2021.3062615

voltage applied to the PIN diodes on an element becomes different, the electromagnetic response of this element, i.e., the phase shift, varies accordingly.

Denote the amplitude of the transmission and reflection responses of one element by $\Gamma^t$ and $\Gamma^r$, respectively. For simplicity, we assume that no power is dissipated by the RIS elements, i.e., $(\Gamma^t)^2+(\Gamma^r)^2=1$. To meet diverse requirements in 6G, three types of RISs are considered here: reflective, transmissive, and hybrid types. In the following, we will elaborate on the three types.

- **Reflective type**: Each element only reflects the incident signals due to the copper backplane. Therefore, we have $\Gamma^t=0$ and $\Gamma^r=1$ for the reflective type RIS.
- **Transmissive type**: Without the copper backplane, the incident signals can only penetrate the elements, i.e., $\Gamma^r=0$ and $\Gamma^t=1$.
- **Hybrid type**: Similar to the transmissive type, the copper backplane is removed. However, by adjusting RIS structures the induced currents within the RIS can be different, which thus leads to both the reflection and transmission of the incident signals, i.e., $\Gamma^r>0$ and $\Gamma^t>0$. In this letter, we assume that the energy is equally split for transmission and reflection, i.e., $(\Gamma^r)^2=(\Gamma^t)^2=\frac{1}{2}$, which is the most typical implementation of hybrid type RISs.

Define $\varphi^r$ and $\varphi^t$ as the reflection and transmission phase shift of an element, respectively. By combining the amplitudes and phase shifts, the reflection and transmission coefficient of the $(m,n)$-th element can be written as $\Gamma^r_{m,n}=\Gamma^r e^{-j\varphi^r_{m,n}}$ and $\Gamma^t_{m,n}=\Gamma^t e^{-j\varphi^t_{m,n}}$, respectively.

### C. Channel Model

Define $\boldsymbol{H}$ as the channel matrix between the BS and UEs, where $[\boldsymbol{H}]_{s,k}\triangleq h^{(s,k)}$ is the channel gain from the $k$-th antenna of the BS to UE $s$. The channel from antenna $k$ of the BS to UE $s$ is composed of $MN$ RIS-based channels, where the $(m,n)$-th channel represents the channel from antenna $k$ to UE $s$ via the $(m,n)$-th RIS element.

The RIS-based channels are modeled by considering path loss, fast fading, and RIS responses. Specifically, the $(m,n)$-th RIS-based channel can be written as

$$\hat{h}^{(s,k)}_{m,n}=\sqrt{\beta^{(s,k)}_{m,n}}\,g^{(s,k)}_{m,n}\Gamma^{(s)}_{m,n}, \tag{1}$$

where $\beta^{(s,k)}_{m,n}$ represents the pathloss, $g^{(s,k)}_{m,n}$ is the small scale fading coefficient with zero mean and unit variance, which are assumed to be independent for different RIS-based channels, and $\Gamma^{(s)}_{m,n}$ represents the RIS element response, where $\Gamma^{(s)}_{m,n}=\Gamma^r_{m,n}$ when the BS and UE $s$ are on the same side of the RIS, and $\Gamma^{(s)}_{m,n}=\Gamma^t_{m,n}$ when they are separated by the RIS. Based on the results in [8], the pathloss can be modeled as

$$\beta^{(s,k)}_{m,n}=\frac{\lambda^2 G l_M l_N}{64\pi^3}\frac{G_I F^{(k)}_{m,n}F^{(s)}_{m,n}}{(D^{(k)}_{m,n}d^{(s)}_{m,n})^{\alpha}}, \tag{2}$$

where $\lambda$ is the wavelength corresponding to the carrier frequency, $G$ is the antenna gain, $\alpha$ represents the pathloss exponent, $F^{(k)}_{m,n}$ is the normalized power radiation pattern of the $(m,n)$-th RIS element for the arrival signal from the $k$-th BS antenna, $F^{(s)}_{m,n}$ is the normalized power radiation pattern of the $(m,n)$-th RIS element for the departure signal to UE $s$, $G_I$ is the antenna gain of one RIS element, and $D^{(k)}_{m,n}$ and $d^{(s)}_{m,n}$ are the distance between antenna $k$ and the $(m,n)$-th RIS element, and the distance between the $(m,n)$-th RIS element and UE $s$, respectively. Define $\theta^{(k)}_{m,n}$ as the angle between the incident signal and the $y$-axis. According to the results in [9], the departure angle has no influence on an RIS-based channel while the effect of the incident angle can be modeled by $\cos\theta^{(k)}_{m,n}$, and thus, $F^{(k)}_{m,n}$ and $F^{(s)}_{m,n}$ can be modeled by

$$F^{(k)}_{m,n}=\cos^2\theta^{(k)}_{m,n}, \tag{3}$$

$$F^{(s)}_{m,n}=\begin{cases}\epsilon_r, & \text{UE } s \text{ is in the reflection zone,}\\ \epsilon_t, & \text{otherwise,}\end{cases} \tag{4}$$

respectively, where $\epsilon_r$ and $\epsilon_t$ are constants related to the hardware implementation.

By combining these RIS-based channels, the channel from antenna $k$ of the BS to UE $s$ can be written as

$$h^{(s,k)}=\sum_{m,n}\hat{h}^{(s,k)}_{m,n}=\sqrt{\hat{\beta}^{(s)}}\sum_{m,n}g^{(s,k)}_{m,n}\Gamma^{(s)}_{m,n}, \tag{5}$$

where $\hat{\beta}^{(s)}$ is average pathloss between UE $s$ and the BS.[1]

## III. Analysis on Sum Rate

According to the results in [10], the additive white Gaussian noise (AWGN) channel capacity can be achieved by dirty paper coding, and the AWGN capacity is given by

$$C=\mathbb{E}\Big(\sum_s\log_2(1+\frac{P_T}{\sigma^2}\Lambda_s[\boldsymbol{H}\boldsymbol{H}^{\mathrm{H}}]_{s,s})\Big), \tag{6}$$

where $P_T$ is the transmit power of the BS, $\sigma^2$ represents the noise variance, and $\Lambda_s$ is the $s$-th element of power allocation vector $\boldsymbol{\Lambda}$, with $\sum_s\Lambda_s=1$.

In the following, an upper bound on the system capacity will be presented. Before presenting the upper bound, we first give a proposition concerning the channel.

**Proposition 1:** *When the number of RIS elements $MN$ is large, and the phase shifts $\varphi^t_{m,n}$ and $\varphi^r_{m,n}$ of the RIS elements are deterministic, we have*

$$\Big(\sum_{m,n}g^{(s,k)}_{m,n}\Gamma^{(s)}_{m,n}\Big)/\sqrt{MN}\sim\mathcal{CN}(0,|\Gamma^{(s)}_{m,n}|^2). \tag{7}$$

*Proof:* Note that the small scale fading coefficients for different RIS elements are independent and identically distributed (i.i.d.). Therefore, when the phase shifts of the RIS elements are given, according to the central limit theorem, the channel gain corresponding to one link from the BS antennas to the UEs follows a complex normal distribution when the number of RIS elements is large.

Since the mean of the small scale fading is 0, the Gaussian distribution has zero mean. Moreover, the variance for the small scale fading is 1 and the amplitude of the RIS response is $|\Gamma^{(s)}_{m,n}|$. Therefore, the variance of the Gaussian distribution is $|\Gamma^{(s)}_{m,n}|^2$. □

Based on the proposition, we can derive an upper bound for the system capacity, as shown in the following proposition.

**Proposition 2:** *The capacity can be upper bounded by*

$$C\le\sum_s\log_2\left(1+\frac{P_T}{\sigma^2}\Lambda_s\hat{\beta}^{(s)}K_tMN|\Gamma^{(s)}_{m,n}|^2\right)\triangleq C^{ub}. \tag{8}$$

*Proof:* According to Jensen's inequality, we have

$$\begin{aligned}C&\le\sum_s\log_2\left(1+\frac{P_T}{\sigma^2}\Lambda_s\mathbb{E}([\boldsymbol{H}\boldsymbol{H}^{\mathrm{H}}]_{s,s})\right)\\&=\sum_s\log_2\left(1+\frac{P_T}{\sigma^2}\Lambda_s\mathbb{E}(\sum_k|h^{(s,k)}|^2)\right).\end{aligned} \tag{9}$$

[1]We assume that the distance between the BS and the RIS is much larger than the size of the antenna array at the BS and the size of the RIS. Moreover, the distance between the BS and UE $s$ is also assumed to be much larger than the size of the RIS. Therefore, the pathloss between UE $s$ and different antennas via different RIS elements can be regarded as the same.

Based on the expression of channel gain in (5), we have

$$\mathbb{E}\Big(\sum_k |h^{(s,k)}|^2\Big) = \sum_k \hat{\beta}^{(s)} \mathbb{E}\Big(\Big|\sum_{m,n} g_{m,n}^{(s,k)} \Gamma_{m,n}^{(s)}\Big|^2\Big). \quad (10)$$

Besides, according to Proposition 1, it can be obtained that

$$\mathbb{E}\Big(\Big|\sum_{m,n} g_{m,n}^{(s,k)} \Gamma_{m,n}^{(s)}\Big|^2\Big) = MN\Big|\Gamma_{m,n}^{(s)}\Big|^2. \quad (11)$$

By combining (10) and (11), we can derive that

$$\mathbb{E}\Big(\sum_k |h^{(s,k)}|^2\Big) = \hat{\beta}^{(s)} K_t MN |\Gamma_{m,n}^{(s)}|^2, \quad (12)$$

which ends the proof. □

**Remark 1:** *$C^{ub}$ is achieved when the eigenvalues of $\boldsymbol{H}\boldsymbol{H}^{\mathbb{H}}$ are the same, which can be obtained by optimizing the phase shifts to maximize the effective rank of $\boldsymbol{H}$ [11].*

In the following, the upper bound $C^{ub}$ given in Proposition 2 is selected to evaluate the performance of different RIS types. Since the distances between the UEs and the RIS will influence the system performance, the distances between the UEs (in both $\mathcal{S}_T$ and $\mathcal{S}_R$) and the RIS are assumed to be the same for simplicity. Moreover, since we evaluate the long-term performance, the small scale fading is neglected when allocating the power. Under these assumptions, the power will be allocated in the following way.

**For the transmissive (reflective) type**, on the one hand, the UEs in $\mathcal{S}_R$ ($\mathcal{S}_T$) will not be allocated power to optimize the system performance. On the other hand, since the data rate is a concave function with respect to the transmit power, an equal power allocation among the UEs subjected to a total power budget will lead to the maximum system capacity. Therefore, the transmit power for UEs in $\mathcal{S}_T$ ($\mathcal{S}_R$) should be the same.

**For the hybrid type**, the transmit power is allocated equally to UEs on the same side of the RIS. Define $\Lambda_R$ and $\Lambda_T$ as the power allocations for UEs in $\mathcal{S}_R$ and $\mathcal{S}_T$, respectively, i.e., $\Lambda_s = \Lambda_R, s \in \mathcal{S}_R$, and $\Lambda_s = \Lambda_T, s \in \mathcal{S}_T$. Due to the constraint $\sum_s \Lambda_s = 1$, $\Lambda_T$ can be expressed as $\Lambda_T = \frac{1 - S_R \Lambda_R}{S_T}$. Therefore, the system capacity $C^{ub}$ is a function of a single variable $\Lambda_R$, where the optimal power allocation can be expressed as

$$\Lambda_s = \begin{cases} \Lambda^*, \text{ UE } s \text{ is in } \mathcal{S}_R, \\ \frac{1 - S_R \Lambda^*}{S_T}, \text{ otherwise.} \end{cases} \quad (13)$$

Here, $\Lambda^* = \max\Big(0, \min\Big(\frac{1}{S_R}, L\frac{2S_T}{S}(\frac{1}{\epsilon_t} - \frac{1}{\epsilon_r}) + \frac{1}{S}\Big)\Big)$, and $L$ is given by $L = 64\pi^3 (D_c^{(c)} d_{c,U})^\alpha \sigma^2 / (P_T \lambda^2 G l_M l_N G_I \cos^2\theta_c^{(c)} K_t MN)$, where $D_c^{(c)}$ is the distance between the center of the BS antenna array and the center of the RIS, $d_{c,U}$ denotes the distance between the center of the RIS and one UE, and $\theta_c^{(c)}$ is the angle between the $y$-axis and an incident signal from the center of the BS antenna array.

With the above power allocation scheme, the sum-rate $C^{ub}$ with these three types of RISs can be expressed as

$$C_R = S_R \log_2\left(1 + \frac{\epsilon_r}{L S_R}\right), C_T = S_T \log_2\left(1 + \frac{\epsilon_t}{L S_T}\right), \quad (14)$$

$$C_H = S_T \log_2\left(1 + \frac{\epsilon_t}{2L}\frac{1 - S_R\Lambda^*}{S_T}\right) + S_R \log_2\left(1 + \frac{\epsilon_r \Lambda^*}{2L}\right). \quad (15)$$

## IV. Type Selection for the RIS

### A. Reflective Versus Transmissive

Denote the function between the sum-rate with type $X$ ($X$ could be $T$, $R$, or $H$) and number $S_T$ of UEs by $C_X(S_T)$. To compare the reflective type with the transmissive type, we first show the trend of $C_R$ and $C_T$ with respect to $S_T$ in the following proposition.

**Proposition 3:** *When $S_T$ increases, the sum-rate $C_T$ increases while $C_R$ decreases.*

*Proof:* To show that $C_T$ is positively correlated with $S_T$, we consider the derivative of $C_T(S_T)$ within $(1, S-1)$, i.e.,

$$C_T'(S_T) = \frac{\left(1 + \frac{\epsilon_t}{L}\frac{1}{S_T}\right)\left(\ln(2)\log_2\left(1 + \frac{\epsilon_t}{L}\frac{1}{S_T}\right) - 1\right) + 1}{\ln(2)\left(1 + \frac{\epsilon_t}{L}\frac{1}{S_T}\right)}. \quad (16)$$

Define $f(x) = x(\ln(2)\log_2(x) - 1) + 1$. It can be shown that $f(x) > 0$ when $x \in (1, \infty)$, and thus, $C_T'(S_T)$ is always positive, which indicates that $C_T$ increases with $S_T$.

Similarly, we can prove that $C_R$ decreases with $S_T$. Due to the space limitations, the proof is omitted here. □

Assume that the power radiation pattern $F_{m,n}^{(s)}$ is approximately isotropic, i.e., $\epsilon_t \approx \epsilon_r$, and we can know that $C_T(1) - C_R(1) \leq 0$ while $C_T(S-1) - C_R(S-1) \geq 0$. Therefore, combined with Proposition 3, we can further obtain that the UE distribution leading to the same performance for the reflective type and transmissive type is unique, which is denoted by $S_T^{(c)}$, i.e., $C_T(S_T^{(c)}) = C_R(S_T^{(c)})$. Based on the monotonicity of $C_T$ and $C_R$, we can conclude that *the transmissive type outperforms the reflective type when $S_T > S_T^{(c)}$, while the reflective type is better when $S_T \leq S_T^{(c)}$.*

To derive the optimal type, the one with higher sum-rate between the reflective and transmissive types will be compared with the hybrid type in the following. Based on the above analysis, the discussions are naturally divided into two parts, i.e., $S_T \leq S_T^{(c)}$ and $S_T > S_T^{(c)}$, where the reflective and the transmissive types are compared with the hybrid type, respectively.

### B. Hybrid Versus Reflective

First, we would like to simplify the expression for $C_H$. Since $\epsilon_t \approx \epsilon_r$, $L\frac{2S_T}{S}\left(\frac{1}{\epsilon_t} - \frac{1}{\epsilon_r}\right) + \frac{1}{S}$ can be approximated by $\frac{1}{S}$. Note that $\frac{1}{S}$ is upper and lower bounded by $\frac{1}{S_R}$ and 0, respectively. Therefore, $C_H$ can be simplified by rewriting $\Lambda^*$ as

$$\Lambda^* = L\frac{2S_T}{S}\left(\frac{1}{\epsilon_t} - \frac{1}{\epsilon_r}\right) + \frac{1}{S}, \quad (17)$$

To compare the hybrid type with the reflective type, we will examine the trend of $C_R - C_H$ with respect to $S_T$ in the following. Assume a sufficiently high transmit SNR $\frac{P_T}{\sigma^2}$ such that when the RIS is of the hybrid type, the received SNR of the UEs is large, i.e., $\frac{P_T}{\sigma^2}\Lambda_s \hat{\beta}^{(s)} K_t MN |\Gamma_{m,n}^{(s)}|^2 \gg 1$. Then, we have the following remark,

**Remark 2:** *The derivative of $C_R(S_T)$ is much larger than that of $C_H(S_T)$, i.e., $|C_R'(S_T)| \gg |C_H'(S_T)|$.*

Remark 2 indicates that $C_R'(S_T) - C_H'(S_T)$ can be approximated by $C_R'(S_T)$. Moreover, Proposition 3 shows that $C_R$ is negatively correlated with $S_T$, and thus, we can conclude that $C_R - C_H$ also decreases with $S_T$.

Due to the monotonicity of $C_R - C_H$, the values of $C_R - C_H$ at $S_T = 1$ and $S_T = S_T^{(c)}$ have an influence on the performance of the reflective type and hybrid type. Specifically, define $C_{eq}$ as the sum-rate with the reflective (transmissive) type RIS when $S_T^{(c)}$ UEs are located within the transmission zone, i.e., $C_{eq} \triangleq C_R(S_T^{(c)}) = C_T(S_T^{(c)})$, and we have, 1) when $C_R(1) - C_H(1) \geq 0$ and $C_{eq} - C_H(S_T^{(c)}) \geq 0$, the reflective type is better than the hybrid type, 2) when

TABLE I
OPTIMALITY CONDITIONS FOR RIS TYPES

| Conditions | | | Optimal type |
|---|---|---|---|
| Sum rate comparison for hybrid and reflective types when $S_T = S_T^{(c)}$ | Sum rate comparison for hybrid and reflective types when $S_T = 1$, and that for hybrid and transmissive types when $S_T = S - 1$ | Number of UEs within the transmission zone | |
| $C_H(S_T^{(c)}) \le C_{eq}$ | \ | $S_T > S_T^{(c)}$ | T |
| | \ | $S_T \le S_T^{(c)}$ | R |
| $C_H(S_T^{(c)}) > C_{eq}$ | $C_H(1) > C_R(1)$, and $C_H(S-1) > C_T(S-1)$ | \ | H |
| | $C_H(1) > C_R(1)$, and $C_H(S-1) \le C_T(S-1)$ | $S_T \ge S_T^{(b)}$ | T |
| | | $S_T < S_T^{(b)}$ | H |
| | $C_H(1) \le C_R(1)$, and $C_H(S-1) > C_T(S-1)$ | $S_T \le S_T^{(a)}$ | R |
| | | $S_T > S_T^{(a)}$ | H |
| | $C_H(1) \le C_R(1)$, and $C_H(S-1) \le C_T(S-1)$ | $S_T \le S_T^{(a)}$ | R |
| | | $S_T \in (S_T^{(a)}, S_T^{(b)})$ | H |
| | | $S_T \ge S_T^{(b)}$ | T |

$C_R(1) - C_H(1) < 0$ and $C_{eq} - C_H(S_T^{(c)}) < 0$, the hybrid type outperforms the reflective type, and 3) when $C_R(1) - C_H(1) \ge 0$ and $C_{eq} - C_H(S_T^{(c)}) < 0$, the reflective type is better if $S_T \in [1, S_T^{(a)}]$, while the hybrid type achieves a larger sum-rate if $S_T \in (S_T^{(a)}, S_T^{(c)}]$. Here, $S_T^{(a)}$ is the unique UE distribution leading to the same performance for the reflective and hybrid types. It is worthwhile noting that $C_{eq} - C_H(S_T^{(c)})$ cannot take positive values when $C_R(1) - C_H(1) < 0$, since $C_R - C_H$ decreases with $S_T$.

### C. Hybrid Versus Transmissive

Similar to Remark 2, it can be proved that $|C_T'(S_T)| \gg |C_H'(S_T)|$, and thus, according to Proposition 3, $C_T - C_H$ increases with $S_T$. As a result, the values of $C_T - C_H$ at $S_T = S_T^{(c)}$ and $S_T = S - 1$ also have an effect on the performance of the hybrid and transmissive types. Based on above discussions, the optimality conditions for each type can be summarized in Table I, where $T$, $R$, and $H$ represent transmissive, reflective, and hybrid type, respectively, and $S_T^{(b)}$ is the unique UE distribution leading to the same performance for the transmissive and hybrid types.

We would like to point out that the number $(M, N)$ of RIS elements, distance $D_c^{(c)}$ between the BS and the RIS, and distance $d_{c,U}$ between the RIS and UEs will influence the relationships among $(C_H(1), C_R(1))$, $(C_H(S-1), C_T(S-1))$, and $\left(C_{eq}, C_H(S_T^{(c)})\right)$, which can change the optimal type. The effects of $(M, N)$ and $(D_c^{(c)}, d_{c,U})$ on the optimal type are given in the following propositions.

**Proposition 4:** *Given the number of RIS elements, when both the UEs and the BS are far from the RIS, the hybrid type is always inferior to the reflective or transmissive type.*

*Proof:* See Appendix VIII. □

**Proposition 5:** *When the number of RIS elements is sufficiently large, i.e., $MN > E_0 2^{\max(E_R, E_T)}$, the hybrid type is always better than the other two types for an arbitrary UE distribution. Here,*

$$E_0 = 64\pi^3 (D_c^{(c)} d_{c,U})^\alpha \sigma^2 / (P_T \lambda^2 G l_M l_N G_I \cos^2 \theta_c^{(c)} K_t),$$
$$E_R = (S - S_T \log_2 \epsilon_r + S \log_2 S - S_R \log_2 S_R)/S_T,$$
$$E_T = (S - S_R \log_2 \epsilon_t + S \log_2 S - S_T \log_2 S_T)/S_R.$$

*Proof:* It is demonstrated in Appendix VIII that

$$C_H - C_T \approx -S + S_R \log_2 \epsilon_t - S_R \log_2 L - (S \log_2 S - S_T \log_2 S_T). \quad (18)$$

By substituting the expression for $L$, we can show that the hybrid type outperforms the transmissive type only when $MN > E_0 2^{E_T}$. Moreover, it can be proved that the hybrid type achieves a higher sum rate than the reflective type only when $MN$ exceeds $E_0 2^{E_R}$, which ends the proof. □

## V. SIMULATION RESULTS

In this section, we verify the validity of the derivation and the proposed optimality conditions by simulations. The parameters are based on 3GPP documents [12] and existing works [7], [13]. Specifically, the RIS is placed vertical to the ground, with one of its edges parallel to the ground. Further, the RIS is deployed vertical to the direction from the BS to the RIS. The height of the BS antennas and RIS center are set as 30 m and 15 m, respectively. The BS is equipped with $K_t = 12$ antennas with a transmit power of $P_T = 43$ dBm. The wavelength is set as $\lambda = 0.1$ m and the noise variance is $\sigma^2 = -96$ dBm. The antenna gain and pathloss exponent are given by $G = 1$ and $\alpha = 2$, respectively. We set the size of one RIS element as $l_M = l_N = 0.02$ m. Additionally, the power radiation parameters of one element are given by $\epsilon_r = 1$ and $\epsilon_t = 0.95$, with the antenna gain of one element $G_I = 1$.

Fig. 2(a) shows the system capacity versus transmit power of the BS. The simulated and analytical results correspond to the data rate $C$ and its upper bound $C^{ub}$, respectively, where the simulated results are obtained by averaging over 100 Monte Carlo simulations. From Fig. 2(a), we can see that $C$ is upper bounded by $C^{ub}$ for the three types, which verifies Proposition 2. Furthermore, according to Fig. 2(a), the gap between the capacity and its upper bound is small, which justifies the selection of $C^{ub}$ as the performance metric for the three types.

Fig. 2(b) depicts the system capacity versus number of UEs within the transmission zone $S_T$, under different distances $\left(d_{c,U}, D_c^{(c)}\right)$. We can see that despite the values of $\left(d_{c,U}, D_c^{(c)}\right)$, the capacity in the reflective type always decreases with $S_T$ while the sum-rate achieved by the transmissive type is positively correlated with $S_T$, which is consistent with Proposition 3. Moreover, from Fig. 2(b), it can be observed that when both distances are set at 200 m, the hybrid type is always inferior to the reflective or transmissive type, which is consistent with Proposition 4. According to Fig. 2(b), we can also find that when both the UEs and the BS are closer

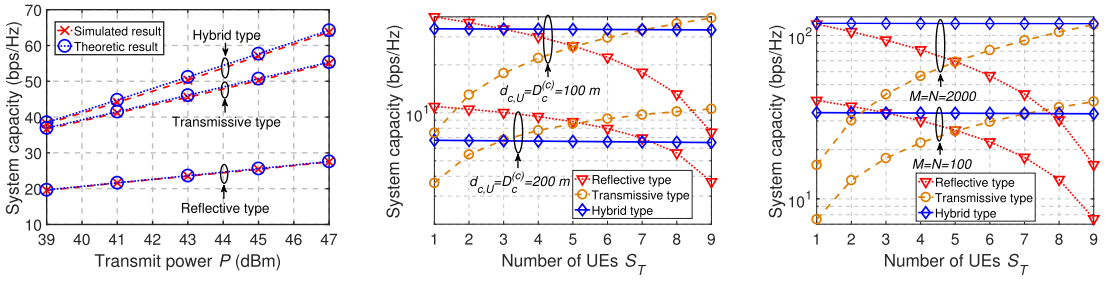


Fig. 2. Simulation results: (a) System capacity vs. transmit power with $S_T=7$, $S=10$, $M=N=50$, and $d_{c,U}=D_c^{(c)}=50$ m. (b) System capacity vs. number of UEs within the transmission zone $S_T$, with $M=N=100$ and $S=10$. (c) System capacity vs. number of UEs within the transmission zone $S_T$, with $d_{c,U}=D_c^{(c)}=100$ m and $S=10$.

to the RIS, the advantage of the hybrid type over the other two types becomes more significant.

Fig. 2(c) shows the system capacity versus $S_T$, under different RIS sizes $(M,N)$. From Fig. 2(c), we can observe that when the RIS contains more elements, the advantage of the hybrid type over the other two types is more significant, since more UEs are scheduled when the hybrid type RIS is adopted. In addition, according to Fig. 2(c), it can be seen that when the number of RIS elements is sufficiently large, the hybrid type always outperforms the other two types for arbitrary $S_T$, which is consistent with Proposition 5.

## VI. Conclusion

In this letter, we have considered a downlink RIS-assisted network with one BS and multiple UEs. The system capacity of this network has been derived, based on which the optimal type of RIS under a specific UE distribution has been analyzed. From the analysis and simulation, we can conclude that: 1) when both the BS and the UEs are far away from the RIS, the hybrid type is always inferior to the reflective or transmissive type; and 2) when the number of RIS elements exceeds the derived threshold, the hybrid type is always better than the other types for an arbitrary UE distribution.

## VII. Proof of Remark 2

Define $A_1=\frac{\epsilon_r}{\epsilon_t}-1$ and $A_2=1-\frac{\epsilon_t}{\epsilon_r}$, and we have

$$C_H'(S_T)=\left(-\log_2\left(1+\frac{\epsilon_r}{2L}\Lambda^*\right)+\log_2\left(1+\frac{\epsilon_t}{2L}\frac{1-S_R\Lambda^*}{S_T}\right)\right)+\left(\frac{S_R}{S}\frac{A_1}{\ln 2\left(1+\frac{\epsilon_r}{2L}\Lambda^*\right)}+\frac{S_T}{S}\frac{A_2}{1+\frac{\epsilon_t}{2L}\frac{1-S_R\Lambda^*}{S_T}}\right)\triangleq E_1+E_2.$$

In the following, it will be proved that $E_1\approx 0$ and $E_2\approx 0$, which indicates that $C_H'(S_T)\approx 0$. Since $\epsilon_t\approx\epsilon_r$, we have $A_1\approx 0$ and $A_2\approx 0$. Furthermore, since $\frac{S_T}{S}<1$, $\frac{S_R}{S}<1$, and the received SNR at each UE with the hybrid type is sufficiently large, we can obtain that $E_2\approx 0$. By substituting the expression for $\Lambda^*$, we have $1+\frac{\epsilon_r}{2L}\Lambda^*=1+\frac{\epsilon_r}{2LS}+\frac{S_T}{S}A_1$. Since $1+\frac{\epsilon_r}{2L}\Lambda^*\gg 1$ while $\frac{S_T}{S}A_1\approx 0$, we can obtain $\log_2\left(1+\frac{\epsilon_r}{2L}\Lambda^*\right)\approx\log_2\left(\frac{\epsilon_r}{2LS}\right)$. Similarly, it can be shown that $\log_2\left(1+\frac{\epsilon_t}{2L}\frac{1-S_R\Lambda^*}{S_T}\right)\approx\log_2\left(\frac{\epsilon_t}{2LS}\right)$. Therefore, $E_1$ can be rewritten as $E_1=\log_2\left(\frac{\epsilon_t}{\epsilon_r}\right)$, from which we have $E_1\approx 0$.

Furthermore, according to (16), it can be seen that the value of $C_T'(S_T)$ is large, which ends the proof.

## VIII. Proof of Proposition 4

We first show that $C_H$ is smaller than $C_T$ for any given $S_T$. Specifically, $C_H-C_T$ can be approximated by

$$\begin{aligned}C_H-C_T&\approx S\log_2\left(\frac{\epsilon_t}{2LS}\right)-S_T\log_2\left(\frac{\epsilon_t}{LS_T}\right)\\&=-S+S_R\log_2\epsilon_t-S\log_2 S\\&\quad+S_T\log_2 S_T-S_R\log_2 L.\end{aligned}\tag{19}$$

Since both the UEs and the BS are far away from the RIS, $L$ takes a large value. Moreover, the other terms in (19) are not influenced by distances $D_c^{(c)}$ and $d_{c,U}$. Therefore, we have $C_H-C_T<0$, and thus, the hybrid type is inferior to the transmissive type, which ends the proof.

## References


[1] M. A. ElMossallamy *et al.*, "Reconfigurable intelligent surfaces for wireless communications: Principles, challenges, and opportunities," *IEEE Trans. Cognit. Commun. Netw.*, vol. 6, no. 3, pp. 990–1002, Sep. 2020.

[2] Y. B. Li *et al.*, "Transmission-type 2-bit programmable metasurface for single-sensor and single-frequency microwave imaging," *Sci. Rep.*, vol. 6, no. 1, pp. 1–8, Mar. 2016.

[3] S. Zhang *et al.*, "Beyond intelligent reflecting surfaces: Reflective-transmissive metasurface aided communications for full-dimensional coverage extension," *IEEE Trans. Veh. Technol.*, vol. 69, no. 11, pp. 13905–13909, Nov. 2020.

[4] X. Wang *et al.*, "Simultaneous realization of anomalous reflection and transmission at two frequencies using bi-functional metasurfaces," *Sci. Rep.*, vol. 8, no. 1, pp. 1–8, Jan. 2018.

[5] B. Zheng and R. Zhang, "Intelligent reflecting surface-enhanced OFDM: Channel estimation and reflection optimization," *IEEE Wireless Commun. Lett.*, vol. 9, no. 4, pp. 518–522, Apr. 2020.

[6] B. Zheng *et al.*, "Intelligent reflecting surface assisted multi-user OFDMA: Channel estimation and training design," *IEEE Trans. Wireless Commun.*, vol. 19, no. 12, pp. 8315–8329, Dec. 2020.

[7] B. Di *et al.*, "Hybrid beamforming for reconfigurable intelligent surface based multi-user communications: Achievable rates with limited discrete phase shifts," *IEEE J. Sel. Areas Commun.*, vol. 38, no. 8, pp. 1809–1822, Aug. 2020.

[8] W. Tang *et al.*, "Wireless communications with reconfigurable intelligent surface: Path loss modeling and experimental measurement," *IEEE Trans. Wireless Commun.*, vol. 20, no. 1, pp. 421–439, Jan. 2021.

[9] O. Ozdogan *et al.*, "Intelligent reflecting surfaces: Physics, propagation, and pathloss modeling," *IEEE Wireless Commun. Lett.*, vol. 9, no. 5, pp. 581–585, May 2020.

[10] D. Tse and P. Viswanath, *Fundamentals of Wireless Communications*. Cambridge, U.K.: Cambridge Univ. Press, 2005.

[11] H. Zhang *et al.*, "Reconfigurable intelligent surface assisted multi-user communications: how many reflective elements do we need?" *IEEE Wireless Commun. Lett.*, early access, Feb. 11, 2021, doi: 10.1109/LWC.2021.3058637.

[12] *Study on New Radio Access Technology: Radio Frequency (RF) and Coexistence Aspects Release 14*, document 3GPP TR 38.803, Sept. 2017.

[13] S. Lin *et al.*, "Reconfigurable intelligent surfaces with reflection pattern modulation: Beamforming design and performance analysis," *IEEE Trans. Wireless Commun.*, vol. 20, no. 2, pp. 741–754, Feb. 2021.